

Cite this: *J. Mater. Chem. B*, 2022, 10, 2699

# Photoinduced immobilization of 2-methacryloyloxyethyl phosphorylcholine polymers with different molecular architectures on a poly(ether ether ketone) surface†

Kyoko Fukazawa,<sup>‡</sup> Mingwei Mu,<sup>b</sup> Sheng-Han Chen<sup>a</sup> and Kazuhiko Ishihara<sup>‡\*</sup>

Poly(ether ether ketone) (PEEK) has seen increasing use in biomedical fields as a replacement for metal implants. Accordingly, the surface functionalities of PEEK are important for the development of medical devices. We have focused on the application of photoinduced reactions in PEEK to immobilize a functional polymer *via* radical generation on the surface, which can react with hydrocarbon groups. In this study, we used zwitterionic copolymers comprising 2-methacryloyloxyethyl phosphorylcholine (MPC) units and *n*-butyl methacrylate (BMA) units with various molecular architectures for surface modification. A random copolymer (poly(MPC-*co*-BMA) (r-PMB)), an AB-type diblock copolymer (di-PMB), and an ABA-type triblock copolymer (tri-PMB) (A segment: poly(BMA); B segment: poly(MPC)) were synthesized with the same monomer compositions. All PMBs were successfully immobilized on the PEEK surface *via* UV irradiation after the dip-coating process, regardless of their molecular structure. In this reaction, the alkyl group of the BMA unit functioned as a photoreactive site on the PEEK surface. This indicates that the molecular structure differences affect the surface properties. For example, compared to r-PMB and tri-PMB, di-PMB-modified surfaces exhibited an extremely low water contact angle of approximately 10°. The findings of this study demonstrate that this surface functionalization method does not require a low-molecular-weight compound, such as an initiator, and can be applied to the surface of inert PEEK through a simple photoreaction under room temperature, atmospheric pressure, and dry state conditions.

Received 5th November 2021,  
Accepted 14th January 2022

DOI: 10.1039/d1tb02415a

rsc.li/materials-b

## 1. Introduction

Polyether ether ketone (PEEK) is a super-engineering plastic with excellent mechanical strength, high thermal stability, and exceptional chemical, water, and radiation resistances.<sup>1,2</sup> In addition to these excellent properties, PEEK has the inherent lightness and workability of plastics. Therefore, PEEK has attracted considerable attention in a wide range of industries, including the medical field, as an alternative to metals.<sup>3–7</sup> In medicine, PEEK is most often used in devices, such as orthopedic, spinal, and cranial implants, because of its excellent

mechanical properties.<sup>8,9</sup> Although neat PEEK has a flexural modulus of 3–4 GPa, its value increases to 18 GPa when it is reinforced with carbon fibers. This value is close to that of cortical bone (7–30 GPa), making PEEK mechanically compatible.<sup>10,11</sup> Recently, three-dimensional (3D) printing technology has made it possible to construct complex PEEK products.<sup>12–14</sup> The development of tailor-made devices will further expand the use of PEEK in the medical field.

Although PEEK has many advantages, its application to the development of medical devices requires improved surface properties, such as hydrophilicity, anti-biofouling, lubricity, and adhesion.<sup>15,16</sup> Oxygen plasma treatment is often used to change the surface properties of materials. After modification, the surface becomes hydrophilic owing to the formation of oxygen-containing functional groups, and the adhesive strength increases with an increase in surface irregularities.<sup>17,18</sup> Oxygen plasma treatment is a powerful method; however, it can strongly affect the bulk material properties, and the types of functional groups introduced are limited.

Grafting functional polymers is a convenient method for introducing various functional groups on PEEK surfaces.

<sup>a</sup> Department of Materials Engineering, School of Engineering, The University of Tokyo, 7-3-1 Hongo, Bunkyo-ku, Tokyo 113-8656, Japan.

E-mail: k.fukazawa@ncvc.go.jp, ishihara@mpc.t.u-tokyo.ac.jp

<sup>b</sup> Department of Bioengineering, School of Food and Bioengineering, Changsha University of Science & Technology, Changsha 410114, China

† Electronic supplementary information (ESI) available. See DOI: 10.1039/d1tb02415a

‡ Department of Biomedical Engineering, National Cerebral and Cardiovascular Center Research Institute (NCVC), 6-1 Kishibe Shin-Machi, Suita, Osaka 564-8565, Japan.

Kyomoto *et al.* first demonstrated photoinduced direct graft polymerization on PEEK surfaces.<sup>19</sup> PEEK has a benzophenone (BP) unit in its main structure. BP is a well-known photoreactive group that generates radicals through photoirradiation. The same photochemical reaction occurs even for a BP unit within the polymer chain. Therefore, PEEK acts as a polymeric photo-initiator for polymerization. Consequently, graft polymerization can be achieved using monomers, and a dense grafting layer can be built on the PEEK surface.<sup>20–23</sup> However, the strict removal of dissolved oxygen in the monomer solution and temperature control are required because the polymerization initiates from the radicals generated on the PEEK surface.

In this study, we explored a convenient process that was performed in an air atmosphere, at room temperature, and under dry conditions. We focused on the hydrogen extraction reaction of radicals generated on PEEK under photoirradiation. If a polymer with hydrocarbon groups is in close contact with the substrate surface, the radicals generated *via* photoirradiation can react with the polymer effectively, and new chemical bonds are formed between the polymer and PEEK surface. Therefore, the PEEK surface can be endowed with diverse functionalities by modifying the polymer properties. Herein, poly(*n*-butyl methacrylate) (PBMA) was used as a source of hydrocarbons. PBMA has a suitable glass transition temperature and provides photoreactive points. Subsequently, 2-methacryloyloxyethyl phosphorylcholine (MPC) was selected to obtain the hydrophilicity and antibiofouling properties. The poly(MPC-*co*-BMA) (PMB) surface is hydrophilic and effectively suppresses protein adsorption and cell adhesion because of the phosphorylcholine group in the side chain of the MPC.<sup>24</sup> PMB coating technology has already been applied to create various medical devices for clinical use.<sup>25</sup> A plausible photo-reaction mechanism for the immobilization of PMB on the PEEK surface is depicted in Fig. 1. The hydrocarbons in the BMA unit are thought to mainly act as photoreactive sites, rather than those in the MPC unit, because the poly(MPC) (PMPC) has a rigid structure. PMPC has a rod-like structure because of the bulky side-chain phosphorylcholine groups that completely cover the methacrylate backbone.<sup>26</sup> Therefore, we synthesized PMB with the same monomer composition and different molecular architectures: a random copolymer (*r*-PMB), an AB-type diblock copolymer (*di*-PMB), and an ABA-type triblock copolymer (*tri*-PMB) (A segment: PBMA; B segment: PMPC). After the photoreaction of PMBs on PEEK, the surface composition, morphology, and thickness were analyzed

using X-ray photoelectron spectroscopy (XPS), atomic force microscopy (AFM), and ellipsometry, respectively. Furthermore, the effects of the polymer architecture on the photoreaction, wettability, and suppression of protein adsorption were investigated.

## 2. Experimental

### 2.1. Materials

A PEEK sheet (APTIV1000 sheet, 100  $\mu\text{m}$  thick) was obtained from Victrex PLC (Lancashire, UK). MPC and Lipidure<sup>®</sup>-PMB (water-soluble random PMB) were purchased from NOF Co., Ltd (Tokyo, Japan), which was synthesized using a previously reported procedure.<sup>27</sup> Additionally, 2,2'-azobisisobutyronitrile (AIBN) was purchased from Kanto Chemical Co., Inc. (Tokyo, Japan). Ethylene bis(2-bromoisoobutyrate) (EBBiB), tris(2-pyridylmethyl) amine (TPMA), and 4-cyano-4-(phenylcarbo-nothiolythio)pentanoic acid (CPA) were purchased from Sigma-Aldrich (St Louis, MO, USA). L-Ascorbic acid, copper(II) bromide ( $\text{CuBr}_2$ ), and albumin from bovine serum (BSA, 019-21272) were obtained from Wako Pure Chemical Industries (Osaka, Japan). All reagents were of extra-pure grade and were used without further purification.

### 2.2. Synthesis of polymers

**2.2.1. Diblock copolymer.** The diblock polymer comprising PMPC and PBMA segments, *di*-PMB, was synthesized using a reversible addition fragmentation chain transfer (RAFT) polymerization technique.<sup>28</sup> The detailed reaction scheme is shown in Fig. S1 (ESI<sup>†</sup>). First, PMPC with 120 MPC units (PMPC prepolymer) was synthesized using AIBN as the initiator and CPA as the chain transfer agent. MPC ( $0.50 \text{ mol L}^{-1}$ ), CPA ( $4.2 \text{ mmol L}^{-1}$ ), and AIBN ( $0.80 \text{ mmol L}^{-1}$ ) were dissolved in methanol at room temperature and bubbled with argon gas for 10 min before sealing the glass tube. Polymerization was performed at  $65^\circ\text{C}$ . After 24 h, 100  $\mu\text{L}$  of the polymer solution was taken from the glass tube and used to evaluate the monomer conversion using proton nuclear magnetic resonance ( $^1\text{H-NMR}$ ). The PMPC prepolymer was precipitated by pouring it into excess diethyl ether/chloroform (80/20 v/v). The precipitated polymer was dried under pressure, dissolved in distilled water, and dialyzed for 3 days using a dialysis membrane with a molecular weight cut-off of 3.5 kDa. Finally, the solvent was removed by freeze-drying to obtain the PMPC prepolymer as a



Fig. 1 Photoreaction mechanism of PMB on a PEEK surface.

light pink powder. The block-type copolymers comprising PMPC and PBMA segments were synthesized using the PMPC prepolymer and AIBN as the macroinitiator and initiator, respectively. The molar ratio of the PMPC prepolymer to BMA was 1:30 for di-PMB. BMA ( $0.50 \text{ mol L}^{-1}$ ), PMPC prepolymer ( $10.4 \text{ mmol L}^{-1}$ ), and AIBN ( $2.0 \text{ mmol L}^{-1}$ ) were dissolved in methanol at room temperature. The glass tube was sealed after bubbling with argon gas for 10 min. Subsequently, polymerization was performed at  $68^\circ \text{C}$  for 24 h. The polymer was precipitated by pouring it into diethyl ether, collected *via* filtration, and then vacuum dried overnight at room temperature.

### 2.3. Triblock copolymer

The triblock polymer (tri-PMB), containing PMPC in the middle segment (B) and PBMA segments (A) on both sides of the polymer chain (ABA), was synthesized using activators regenerated by electron transfer (ARGET)-atom transfer radical polymerization (ATRP). The PMPC prepolymer was prepared as reported previously;<sup>29</sup> the detailed procedure is shown in Fig. S2 (ESI†). The final molar composition of the polymerization reaction was  $[\text{MPC}]/[\text{EBBiB}]/[\text{CuBr}_2]/[\text{TPMA}]/[\text{L-ascorbic acid}] = 120/1.0/0.020/0.40/0.20$ . Polymerization was performed in degassed methanol at  $20^\circ \text{C}$  with stirring. The molar concentration of MPC was  $1.0 \text{ mol L}^{-1}$ . After 5 h,  $100 \mu\text{L}$  of the polymer solution was taken from the glass tube, and the monomer conversion was evaluated using  $^1\text{H-NMR}$ . Thereafter, 30 times the amount of BMA for the PMPC prepolymer was added to the polymer solution under argon gas bubbling, and the second reaction was performed at  $40^\circ \text{C}$  for 24 h. The polymer was precipitated by pouring it into excess diethyl ether/chloroform (80/20 v/v). The precipitated polymer was dried under pressure, dissolved in distilled water, and dialyzed for 3 days using a dialysis membrane with a molecular weight cut-off of 3.5 kDa. Finally, the solvent was removed by freeze-drying to obtain tri-PMB as a white powder.

### 2.4. Surface modification by photoreaction

The PEEK substrates were cleaned using ultrasonication in *n*-hexane, ethanol, and acetone for 10, 10, and 5 min, respectively. Lipidure<sup>®</sup>-PMB (r-PMB), di-PMB, and tri-PMB were dissolved in ethanol to make three 0.50 wt% solutions. Subsequently,  $1.0 \times 1.0 \text{ cm}^2$  PEEK substrates were immersed into each PMB solution using a dip-coating process for 10 s. All samples were dried in an ethanol vapor atmosphere for 10 min at room temperature, followed by UV irradiation ( $365 \text{ nm}$ ,  $18 \text{ mW cm}^{-2}$ ) for 30 min. After photoirradiation, the modified PEEK substrates were immersed and shaken gently in ethanol for 24 h to remove the unreacted polymer. Finally, the PMB-modified PEEK substrates were dried and stored in a vacuum desiccator.

### 2.5. Surface characterization

The thicknesses of the r-PMB layers after the photoreaction with different polymer concentrations and UV irradiation times were measured using an ellipsometer (FE-5000S, Otsuka

Electronics Co., Ltd, Osaka, Japan) to determine the photo-reactive conditions. Moreover, the thicknesses of the di-PMB, tri-PMB, and PBMA layers after the photoreaction at a polymer concentration of 0.50 wt% and UV irradiation time of 30 min were measured. PBMA was used as a control. The measurements were performed under dry conditions using visible light at an incident angle of  $70^\circ$ . All data were analyzed using the Cauchy layer model with an assumed refractive index of 1.49 at 632.8 nm.

XPS (AXIS-His165 Kratos/Shimadzu, Kyoto, Japan) with a non-monochromatic magnesium anode source was used to determine the elemental composition of the PEEK surfaces after the PMB photoreactions. The photoelectron take-off angle was set to  $90^\circ$ . The spectra for C, O, N, and P were recorded. All binding energies were corrected by referencing to the  $\text{C}_{1s}$  peak at 285.0 eV.

The surface morphology of the PEEK substrates after the photoreaction of the PMBs was observed using atomic force microscopy (AFM; Nanoscope IIIa; Nihon Veeco, Tokyo, Japan) operated in the tapping mode. The measurement was performed at a scan rate of 1.0 Hz using a standard cantilever with a spring constant of  $40 \text{ N m}^{-1}$  and a resonant frequency of 300 kHz. The root mean square (RMS) of the surface roughness of a  $5 \times 5 \mu\text{m}^2$  area was calculated using the bundled software. Three positions were measured for each sample.

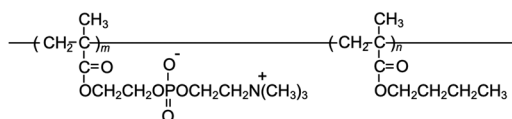
The contact angles of specific liquids were measured under dry conditions using a static contact angle goniometer (SCA; FACE CA-X contact angle meter, Kyowa Interface Science Co. Ltd, Saitama, Japan). Thereafter,  $3 \mu\text{L}$  droplets of water and diiodomethane were placed on the modified PEEK surfaces, and the contact angles were measured within 10 s. Photographic images were used to determine the contact angles. Each sample was measured at five positions. The surface free energy and its dispersion and polar components were calculated using the Owens–Wend equation from the measured static contact angles of water and diiodomethane and the surface free energy of the liquids.<sup>30</sup>

## 3. Results and discussion

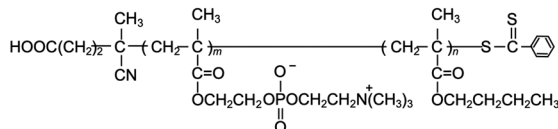
### 3.1. Characterization of PMBs

To evaluate the effect of the molecular architecture on the photoreactivity and surface properties, PMBs with the same monomer composition and different molecular architectures were prepared. Fig. 2 shows the chemical structures of r-PMB, di-PMB, and tri-PMB. Di-PMB and tri-PMB were synthesized using the RAFT polymerization (Fig. S1, ESI†) and ARGET-ATRP (Fig. S3, ESI†) techniques, respectively. The synthesis results are summarized in Table 1. The monomer conversion rate of MPC, which was the first reaction step, was 95% for di-PMB; therefore, the PMPC prepolymer was 114 units. In contrast, the monomer conversion rate of MPC in tri-PMB was 95%, and the resulting PMPC prepolymer was 107 units. For both di-PMB and tri-PMB, the monomer conversion rate of BMA, which was the second reaction, was 100%. Finally, di-PMB and tri-PMB with approximately

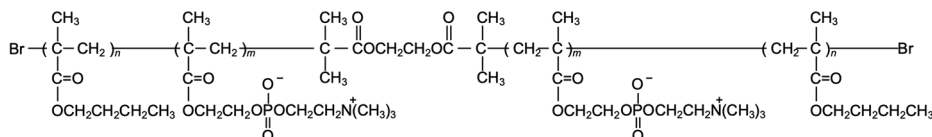
## Random copolymer (Lipidure®-PMB) (r-PMB)



## Diblock copolymer (di-PMB)



## Triblock copolymer (tri-PMB)



Composition  
m: 80 mol%, n: 20 mol%

Fig. 2 Chemical structures of PMBs.

Table 1 Synthetic results of diblock- and triblock-type PMBs

Abb.	Composition (mol%)				$M_n^b$ ( $\times 10^4$ )	$M_w/M_n^c$
	In feed		In copolymer <sup>a</sup>			
	MPC	BMA	MPC	BMA		
di-PMB80	80	20	79	21	3.8	1.2
tri-PMB80	80	20	78	22	3.6	1.4

<sup>a</sup> Determined by <sup>1</sup>H-NMR spectroscopy in ethanol-*d*<sub>6</sub>. <sup>b</sup> Number-averaged molecular weight ( $M_n$ ) was determined by NMR measurements in CD<sub>3</sub>OD. <sup>c</sup> Polydispersity of weight-averaged molecular ( $M_w$ ) and  $M_n$  were determined by GPC measurement in methanol/water mixture (7/3 by volume) containing 10 mM LiBr.

80 mol% MPC units and low polydispersity were successfully synthesized. All PMBs were soluble in alcohol and water.

### 3.2. Photoreaction of PMBs on PEEK substrates

The effects of the polymer concentration and photoirradiation time on the polymer layer thickness were investigated using r-PMB. Fig. 3(a) shows the relationship between the r-PMB layer thickness and polymer concentration for a photoirradiation time of 30 min. When the photoreaction process was performed with 0.10 and 0.50 wt% r-PMB solutions, the thicknesses of the r-PMB layers before washing were approximately 14 and 40 nm, respectively (data not shown). Conversely, the thickness of the r-PMB layer after washing was constant at approximately 8 nm, except when the polymer concentration was 0.10 wt%. BP selectively reacts with C-H bonds within a 3.1 Å radius of the carbonyl oxygen.<sup>31</sup> This indicates that only the polymer chains in contact with the PEEK surface were involved in the photoreaction. Fig. 3(b) shows the relationship between the thickness

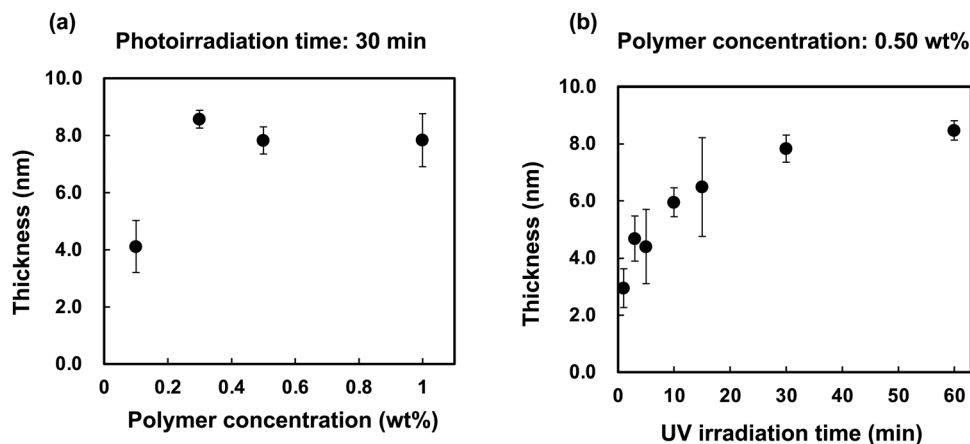


Fig. 3 (a) Relationship between the r-PMB layer thickness and polymer concentration. (b) Relationship between the thickness of the r-PMB layer and photoirradiation time.

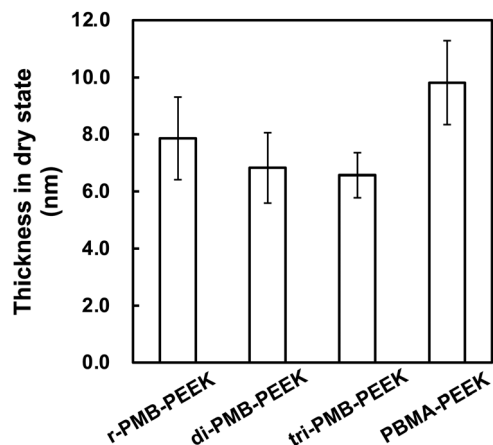


Fig. 4 Thicknesses of the PMB layers after photoreaction.

of the r-PMB layers and the photoirradiation time at a polymer concentration of 0.50 wt%. The thickness of the r-PMB layers increased with the increasing photoirradiation time and reached saturation in 30 min. This result is consistent with the concentration of radicals generated on the PEEK surface,<sup>32</sup> indicating that the density of the immobilized polymer increased over time. The relationship between the UV irradiation time and thickness depends on the radical concentration generated on the PEEK surface; therefore, the trend observed in Fig. 3(b) is expected for all PMBs. The thickness was approximately 8 nm after 30 min of photoirradiation, which agrees with the result shown in Fig. 3(a). When PMPC was used to modify the polymer, the thickness after the photoreaction was

only 4 nm. The hydrocarbons of the BMA unit are thought to act as the main photoreactive sites, rather than those in the MPC unit, because of the bulky side-chain phosphorylcholine groups.<sup>26</sup> Fig. 4 shows the thicknesses of the r-PMB, di-PMB, tri-PMB, and PBMA layers after the photoreaction. The thicknesses of the PMB layers immobilized on the PEEK surface after the photoreaction were almost the same. In contrast, the thickness of the PBMA layer was larger than that of the polymer layers. This is probably because PBMA contains multiple hydrocarbons that react with the PEEK surface.

### 3.3. Surface chemical/morphological characterization of PMB-modified PEEK substrates

The surface was then analyzed using XPS after the photoreaction of the PMBs. Fig. 5 shows the XPS spectra of the untreated PEEK, r-PMB-PEEK, di-PMB-PEEK, and tri-PMB-PEEK surfaces. Strong peaks were observed in the  $C_{1s}$  and  $O_{1s}$  regions of the untreated PEEK substrate surface. The peaks at 285, 286, and 289 eV were assigned to the C–C, C–O, and C=O bonds, respectively. The two peaks at 531 and 533 eV were assigned to the C–O and C=O bonds, respectively. For the r-PMB-PEEK, di-PMB-PEEK, and tri-PMB-PEEK surfaces, the peaks attributed to the MPC unit were observed in the  $N_{1s}$  and  $P_{2p}$  regions. The peak at 403 eV in the  $N_{1s}$  region was assigned to the trimethylammonium group ( $-N^+(\text{CH}_3)_3$ ), while the peak at 134 eV in the  $P_{2p}$  region was assigned to the phosphate ester. Therefore, regardless of the molecular architecture, PMBs were immobilized on the surface of the PEEK substrate by photoreactions. The peaks assigned to the PMBs were still observed



Fig. 5 XPS spectra of (a) untreated PEEK, (b) r-PMB-PEEK, (c) di-PMB-PEEK, and (d) tri-PMB-PEEK surfaces.

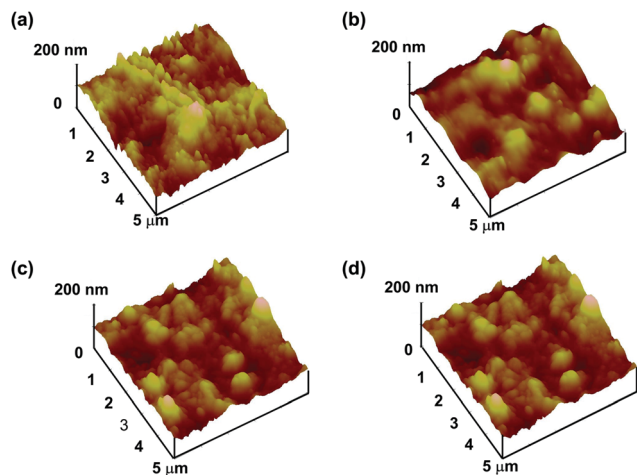


Fig. 6 High-resolution AFM images of (a) untreated PEEK, (b) r-PMB-PEEK, (c) di-PMB-PEEK, and (d) tri-PMB-PEEK surfaces.

on the PEEK surface even after washing with ethanol, which is a good solvent for PMBs. These results indicate that the PMBs were covalently immobilized on the PEEK substrates by photoreactions.

Fig. 6 shows the surface morphology of r-PMB-PEEK, di-PMB-PEEK, and tri-PMB-PEEK measured using AFM in the dry state. The RMS surface roughness of the untreated PEEK substrate was  $18.8 \pm 1.1$  nm, and it demonstrated a relatively large asperity. This was attributed to the manufacturing process. The RMS roughness values of r-PMB-PEEK, di-PMB-PEEK, and tri-PMB-PEEK were  $15.7 \pm 1.9$ ,  $17.7 \pm 1.2$ , and  $19.0 \pm 1.9$  nm, respectively, and exhibited no difference from that of the untreated PEEK substrate. In previous reports, a 100 nm thick PMPC layer was prepared using graft polymerization.<sup>33</sup> Those reports observed a smoother surface compared to the untreated PEEK substrate. Our results using AFM and ellipsometry were consistent with each other, indicating that the PMB layer was extremely thin. No significant morphological differences were observed between r-PMB-PEEK, di-PMB-PEEK, and tri-PEEK in the dry state.

### 3.4. Surface energy characterization of PMB-modified PEEK substrates

The wettability and hydrophilicity depend on the density and type of functional groups on the material surface. The hydrophilicity of the PEEK substrates was evaluated by measuring the water contact angle under dry conditions, and the surface free energy was calculated. The results are shown in Table 2. The water contact angle on the untreated PEEK surface was  $77.8^\circ$ , and the polar ( $\gamma_s^p$ ) and dispersion ( $\gamma_s^d$ ) components were 1.6 and  $43.8$  mJ m<sup>-2</sup>, respectively. This indicates that PEEK is hydrophobic. After 30 min of UV irradiation, the water contact angle decreased owing to the formation of oxygen-containing functional groups on the surface (Fig. S5, ESI†).<sup>34,35</sup> On the surfaces treated with r-PMB, di-PMB, and tri-PMB, the water contact angles were  $42.9^\circ$ ,  $10.2^\circ$ , and  $24.8^\circ$ , respectively; hydrophilicity was imparted from the MPC units. Interestingly, although

Table 2 Contact angles of specific liquids and surface free energies of PEEK substrates after photoreaction with PMBs

Substrate	Contact angles (deg.)		Surface free energy (mJ m <sup>-2</sup> )		
	Water	Diiodomethane	$\gamma_s^p$	$\gamma_s^d$	$\gamma_s$
PEEK (Untreated)	77.8	28.0	1.6	43.8	45.4
PEEK (After UV irradiation)	56.0	31.1	15.3	33.0	48.3
r-PMB-PEEK	42.9	33.9	27.6	27.7	55.3
di-PMB-PEEK	10.2	26.4	46.2	25.6	71.8
tri-PMB-PEEK	24.8	32.6	41.7	24.5	66.3

the amount of MPC units was the same for r-PMB, di-PMB, and tri-PMB, di-PMB-PEEK showed an extremely low water contact angle of  $10.2^\circ$ . The  $\gamma_s^p$  values of r-PMB-PEEK, di-PMB-PEEK, and tri-PMB-PEEK were 27.6, 46.2, and 41.7 mJ m<sup>-2</sup>, respectively. The order of  $\gamma_s^p$  corresponds to the amount of MPC units present on the outermost surface. Note that this measurement was performed in a dry state; therefore, the molecular mobility of the MPC unit at the water interface can affect the water contact angle. As mentioned above, the photoreaction preferentially occurs between the BMA unit and the PEEK surface. Therefore, the difference in the surface free energy is considered to be due to the difference in the binding mode, as shown in Fig. 7. Previously, Kobayashi *et al.* constructed a PMPC polymer brush layer with a dried thickness of 40 nm or more and a graft density of 0.23 chains per nm on silicon substrates using surface-initiated ATRP (SI-ATRP).<sup>36</sup> The surface free energy was evaluated; the values of  $\gamma_s^p$ ,  $\gamma_s^d$ , and  $\gamma_s$  were 41.0, 33.5, and 74.5 mJ m<sup>-2</sup>, respectively. On the di-PMB surface, the values of  $\gamma_s^p$ ,  $\gamma_s^d$ , and  $\gamma_s$  were 46.2, 25.6, and 71.8 mJ m<sup>-2</sup>, respectively. Although di-PMB was immobilized by the photoreaction after the dip-coating process, the surface free energy was close to that of the PMPC brush layer. The surface of di-PMB resembles a polymer brush with one free end. For the polymer brush prepared by SI-ATRP, the graft density was calculated from the thickness determined using ellipsometry and the molecular weight of the polymer chains on the surface, which was determined from the polymerization degree measured using the <sup>1</sup>H-NMR spectrum of the free polymer.<sup>37</sup> However, in this study, PMBs were immobilized on the PEEK surface by the photoreaction after the dip-coating process. The terminal of the polymer chains does not always react with the substrate; hence, it was not possible to determine the PMB density using ellipsometry, as in the SI-ATRP method. In addition, it was difficult to quantify the amount of PMPC chains per unit area using Fourier transform infrared spectroscopy combined with attenuated total reflection equipment (FT-IR/ATR) spectra owing to the thin layer.

The surface free energy is a parameter used to determine the antifouling properties of a material surface. We have previously synthesized photoreactive phospholipid polymers using RAFT polymerization, where the surface modification of *n*-butyl trichlorosilane-immobilized silicon substrates was performed through photoreactions. After modification, the surface became hydrophilic owing to the MPC units, and fibrinogen adsorption and platelet adhesion were effectively suppressed.<sup>38</sup>

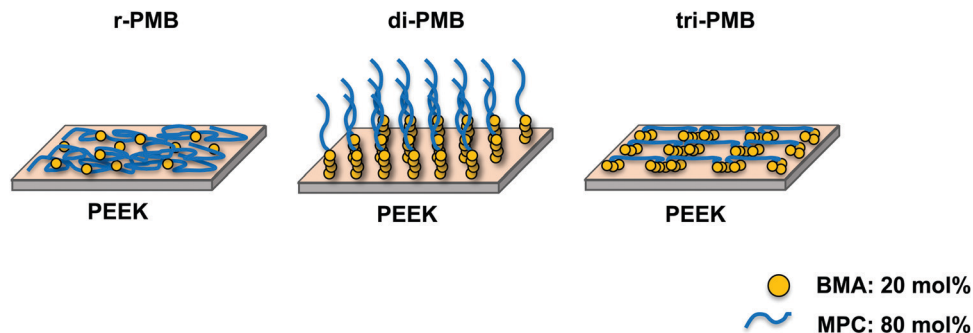


Fig. 7 Schematic of the PEEK surface after the photoreactions of r-PMB, di-PMB and tri-PMB.

The amount of BSA adsorbed on the PEEK substrate after surface modification with PMBs was measured using  $\mu$ BCA (Fig. S6, ESI<sup>†</sup>). BSA adsorption was effectively suppressed after surface modification with PMBs; however, there was no significant difference between r-PMB, di-PMB, and tri-PMB in the evaluation by  $\mu$ BCA. After sufficient equilibration, the PEEK surface is thought to be covered with MPC units, regardless of the polymer architectures. The photoinduced surface treatment of the MPC polymers shown in this study is convenient because it is effective for PEEK substrates and can be performed in air at room temperature. This technology can be applied to the surface functionalization of PEEK medical implants and to improve their compatibility with cells and tissues in the future. More detailed research on these topics is underway.

## 4. Conclusions

Well-defined molecular structures of di-PMB and tri-PMB were successfully synthesized *via* RAFT polymerization and ARGET-ATRP, respectively. We demonstrated that r-PMB, di-PMB, and tri-PMB could be immobilized on the surface of the PEEK substrate using a photoreaction at room temperature under atmospheric conditions. This immobilization was due to the photoinduced radical formation and reactions with hydrocarbon groups in the PMBs. The BMA units of PMB reacted preferentially with the PEEK surface; therefore, r-PMB, di-PMB, and tri-PMB were bound to the PEEK surface by different binding modes. After the surface modification of the PMBs, the surface of the PEEK substrate became hydrophilic owing to the characteristics of the MPC unit. In particular, the performance of the surface depended on the molecular architecture of the PMBs; that is, the di-PMB-PEEK surface was extremely hydrophilic. Because all PMBs had the same number of MPC units, this study revealed that molecular structure differences affect the wettability of the surface. We concluded that photoinduced surface modification with di-PMB could easily modify inert PEEK surfaces to become super-hydrophilic.

## Author contributions

K. F. and K. I. designed the study. K. F., M. M., and S.-H. C. performed the experiments. K. F. wrote the manuscript with

editorial assistance from K. I. All authors have read and approved the final manuscript.

## Conflicts of interest

There are no conflicts to declare.

## Acknowledgements

This research was supported in part by the S-innovation Research Program for the “Development of the biofunctional materials for realization of innovative medicine”, Japan Agency for Medical Research and Development (AMED), and a Grant-in-Aid for Scientific Research for Fostering Joint International Research (18KK0305).

## References

- 1 S. M. Kurtz and J. N. Devine, PEEK biomaterials in trauma, orthopedic, and spinal implants, *Biomaterials*, 2007, **28**, 4845–4869.
- 2 V. Panayotov, V. Orti, F. Cuisinier and J. Yachouh, Polyetheretherketone (PEEK) for medical applications, *J. Mater. Sci.: Mater. Med.*, 2016, **27**, 118.
- 3 P. R. Monich, B. Henriques, A. P. Novaes de Oliveira, J. C. M. Souza and M. C. Fredel, Mechanical and biological behavior of biomedical PEEK matrix composites: a focused review, *Mater. Lett.*, 2016, **185**, 593–597.
- 4 Y. Zhao, H. M. Wong, S. C. Lui, E. Y. Chong, G. S. Wu, X. L. Zhao, C. Wang, H. B. Pan, K. M. Cheung, S. L. Wu, P. K. Chu and K. W. K. Yeung, Plasma surface functionalized polyetheretherketone for enhanced osseointegration at bone-implant interface, *ACS Appl. Mater. Interfaces*, 2016, **8**, 3901–3911.
- 5 T. M. Grupp, H. J. Meisel, J. A. Cotton, J. Schwiesau, B. Fritz, W. Blomer and V. Jansson, Alternative bearing materials for intervertebral disc arthroplasty, *Biomaterials*, 2010, **31**(3), 523–531.
- 6 E. L. Steinberg, E. Rath, A. Shlaifer, O. Chechik, E. Maman and M. Salai, Carbon fiber reinforced PEEK Optima—A composite material biomechanical properties and wear/debris characteristics of CF-PEEK composites for orthopedic

- trauma implant, *J. Mech. Behav. Biomed. Mater.*, 2013, **17**, 221–228.
- 7 M. Punchak, L. K. Chung, C. Lagman, T. T. Bui, J. Lazareff, K. Rezzadeh, R. Jarrahy and I. Yang, Outcomes following polyetheretherketone (PEEK) cranioplasty: systematic review and meta-analysis, *J. Clin. Neurosci.*, 2017, **41**, 30–35.
  - 8 J. M. Toth, M. Wang, B. T. Estes, J. L. Scifert, H. B. Seim III and A. S. Turner, Polyetheretherketone as a biomaterial for spinal applications, *Biomaterials*, 2006, **27**, 324–334.
  - 9 M. Kyomoto, T. Moro, S. Yamane, M. Hashimoto, Y. Takatori and K. Ishihara, Poly(ether-ether-ketone) orthopedic bearing surface modified by self-initiated surface grafting of poly(2-methacryloyloxyethyl phosphorylcholine), *Biomaterials*, 2013, **34**, 7829–7839.
  - 10 H. B. Skinner, Composite technology for total hip arthroplasty, *Clin. Orthop. Relat. Res.*, 1988, **235**, 224–236.
  - 11 T. Kizuki, T. Matsushita and T. Kokubo, Apatite-forming PEEK with TiO<sub>2</sub> surface layer coating, *J. Mater. Sci.: Mater. Med.*, 2015, **26**, 5359.
  - 12 X. Han, N. Sharma, Z. Xu, L. Scheideler, J. Geis-Gerstorfer, F. Rupp, F. M. Thieringer and S. Spintzyk, An in vitro study of osteoblast response on fused-filament fabrication 3D printed PEEK for dental and cranio-maxillofacial implants, *J. Clin. Med.*, 2019, **8**, 771.
  - 13 P. Honigmann, N. Sharma, B. Okolo, U. Popp, B. Msallem and F. M. Thieringer, Patient-specific surgical implants made of 3D printed PEEK: material, technology, and scope of surgical application, *BioMed Res. Int.*, 2018, **2018**, 4520639.
  - 14 X. Feng, L. Ma, H. Liang, X. Liu, J. Lei, W. Li, K. Wang, Y. Song, B. Wang and G. Li, Osteointegration of 3D-printed fully porous polyetheretherketone scaffolds with different pore sizes, *ACS Omega*, 2020, **5**, 26655–26666.
  - 15 H. Nakano, Y. Noguchi, S. Kakinoki, M. Yamakawa, I. Osaka and Y. Iwasaki, Highly durable lubricity of photo-cross-linked zwitterionic polymer brushes supported by poly(ether ether ketone) substrate, *ACS Appl. Bio Mater.*, 2020, **3**, 1071–1078.
  - 16 R. Ding, T. Chen, Q. Xu, R. Wei, B. Feng, J. Weng, K. Duan, J. Wang, K. Zhang and X. Zhang, Mixed modification of the surface microstructure and chemical state of polyetheretherketone to improve its antimicrobial activity, hydrophilicity, cell adhesion, and bone integration, *ACS Biomater. Sci. Eng.*, 2020, **6**, 842–851.
  - 17 N. Inagaki, S. Tasaka, T. Horiuchi and R. Suyama, Surface modification of poly(aryl ether ether ketone) film by remote oxygen plasma, *J. Appl. Polym. Sci.*, 1998, **68**, 271–279.
  - 18 P. Laurens, B. Sadras, F. Decobert, F. Arefi-Khonsari and J. Amouroux, Enhancement of the adhesive bonding properties of PEEK by excimer laser treatment, *Int. J. Adhes. Adhes.*, 1998, **18**, 19–27.
  - 19 M. Kyomoto and K. Ishihara, Self-initiated surface graft polymerization of 2-methacryloyloxyethyl phosphorylcholine on poly(ether ether ketone) by photoirradiation, *ACS Appl. Mater. Interfaces*, 2009, **1**, 537–542.
  - 20 X. D. Zhao, D. S. Xiong, K. Wang and N. Wang, Improved biotribological properties of PEEK by photo-induced graft polymerization of acrylic acid, *Mater. Sci. Eng., C*, 2017, **75**, 777–783.
  - 21 T. Tateishi, M. Kyomoto, S. Kakinoki, T. Yamaoka and K. Ishihara, Reduced platelets and bacteria adhesion on poly(ether ether ketone) by photoinduced and self-initiated graft polymerization of 2-methacryloyloxyethyl phosphorylcholine, *J. Biomed. Mater. Res., Part A*, 2014, **102**, 1342–1349.
  - 22 Y. Zhang, K. Hasegawa, S. Kamo, K. Takagi and A. Takahara, Enhanced adhesion effect of epoxy resin on carbon fiber-reinforced Poly(etheretherketone) via surface initiated photopolymerization of glycidyl methacrylate, *Polymer*, 2020, **209**, 123036.
  - 23 K. Oai, Y. Inoue and K. Ishihara, Antibacterial effect of nanometer-size grafted layer of quaternary ammonium polymer on poly(ether ether ketone) substrate, *J. Appl. Polym. Sci.*, 2020, **137**, 49088.
  - 24 K. Ishihara and K. Fukazawa, Chapter 5, 2-Methacryloyloxyethyl phosphorylcholine polymers, *Phosphorus Based Polymers: from Synthesis to Applications*, ed. S. Monge and G. David, Royal Society of Chemistry, Cambridge, 2014, pp. 68–96.
  - 25 K. Ishihara, Blood-compatible surfaces with phosphorylcholine-based polymers for cardiovascular medical devices, *Langmuir*, 2019, **35**, 1778–1787.
  - 26 K. Ishihara, M. Mu, T. Konno, Y. Inoue and K. Fukazawa, The unique hydration state of poly(2-methacryloyloxyethyl phosphorylcholine), *J. Biomater. Sci., Polym. Ed.*, 2017, 1298278.
  - 27 K. Ishihara, T. Ueda and N. Nakabayashi, Preparation of phospholipid polymers and their properties as polymer hydrogel membranes, *Polym. J.*, 1990, **22**, 355–360.
  - 28 M. Mu, T. Konno, Y. Inoue and K. Ishihara, Solubilization of poorly water-soluble compounds using amphiphilic phospholipid polymers with different molecular architectures, *Colloids Surf., B*, 2017, **158**, 249–256.
  - 29 S. Chantasirichot, Y. Inoue and K. Ishihara, Introduction of functional groups to reactive ABA block-copolymers composed of poly(2-methacryloyloxyethyl phosphorylcholine) and poly(glycidyl methacrylate) for spontaneous hydrogel formation, *Polymer*, 2017, **123**, 100–106.
  - 30 D. K. Owens and R. C. Wendt, Estimation of the surface free energy of polymers, *J. Appl. Polym. Sci.*, 1969, **13**, 1741–1747.
  - 31 E. J. Park, G. T. Carroll, N. J. Turro and J. T. Koberstein, Shedding light on surfaces—using photons to transform and pattern material surfaces, *Soft Matter*, 2009, **5**, 36–50.
  - 32 S. Yamane, M. Kyomoto, T. Moro, M. Hashimoto, Y. Takatori, S. Tanaka and K. Ishihara, Wear resistance of poly(2-methacryloyloxyethyl phosphorylcholine)-grafted carbon fiber reinforced poly(ether ether ketone) liners against metal and ceramic femoral heads, *J. Biomed. Mater. Res., Part B*, 2018, **106**, 1028–1037.
  - 33 T. Shiojima, Y. Inoue, M. Kyomoto and K. Ishihara, High-efficiency preparation of poly(2-methacryloyloxyethyl phosphorylcholine) grafting layer on poly(ether ether ketone) by photoinduced and self-initiated graft polymerization in an aqueous solution in the presence of inorganic salt additives, *Acta Biomater.*, 2016, **40**, 38–45.



- 34 A. G. Shard and J. P. S. Badyal, Surface oxidation of polyethylene, polystyrene, and PEEK: the synthon approach, *Macromolecules*, 1992, **25**, 2053–2054.
- 35 S. Kim, K.-J. Lee and Y. Seo, Polyetheretherketone (PEEK) Surface Functionalization by Low-Energy Ion-Beam Irradiation under a Reactive O<sub>2</sub> Environment and Its Effect on the PEEK/Copper Adhesives, *Langmuir*, 2004, **20**, 157–163.
- 36 M. Kobayashi, Y. Terayama, H. Yamaguchi, M. Terada, D. Murakami, K. Ishihara and A. Takahara, Wettability and antifouling behavior on the surfaces of superhydrophilic polymer brushes, *Langmuir*, 2012, **28**, 7212–7222.
- 37 M. Husseman, E. E. Malmstrom, M. McNamara, M. Mate, D. Mecerreyes, D. G. Benoit, J. L. Hedrick, P. Mansky, E. Huang, T. P. Russell and C. J. Hawker, Controlled synthesis of polymer brushes by living free radical polymerization techniques, *Macromolecules*, 1999, **32**, 1424–1431.
- 38 K. Fukazawa, K. Tsuji, Y. Inoue and K. Ishihara, Direct photoreactive immobilization of water-soluble phospholipid polymers on substrates in an aqueous environment, *Colloids Surf., B*, 2021, **199**, 111507.